

Measurement-based Performance Evaluation of 3D MIMO in High Rise Scenario

Chi Zhang, Lei Tian, Jianhua Zhang, Tao Sun, Chun Pan

Key Laboratory of Universal Wireless Communications, Ministry of Education, Wireless Technology Innovation Institute, Beijing University of Posts and Telecommunications, Beijing, 100876, China
Email: zhangchimy@163.com

Abstract—In this paper, the performance of 3D MIMO is evaluated with measurement data for the first time. The MIMO channel response for different 3D antenna configurations is extracted from measured channel matrix in the high rise scenario and the corresponding data rates are calculated. The major findings are as follows. For single user MIMO, vertically spaced antennas does better in transmit beamforming while horizontally spaced antennas stands out in spatial multiplexing for its wider azimuth angle spread. For multi-user MIMO (MU-MIMO), horizontally distributed antennas performs best when users are on the same floor while the combination of closely spaced vertical antennas with widely spaced horizontal antennas is especially more suitable when users are on different floors. Moreover, it is found that for MU-MIMO, the rate increment comes from increase in BS antenna number is limited but increasing the number of users can improve the sum rate effectively. In addition, it is also noticed selecting users on different floors for 3D MU-MIMO can achieve the best performance.

I. INTRODUCTION

Driven by the rapidly increasing demand for mobile applications, wireless data traffic continue experiencing an explosive increase and even grow more than 1000 times by 2020 [1, 2]. Multi-input multi-output (MIMO) technology is considered as one of the most promising approaches for high data rates and has been introduced into Long Term Evolution (LTE) and LTE-Advanced [3] in the past decade. However, existing MIMO technologies can not meet the requirement of future traffic growth and new MIMO technologies which can further exploit the richness of real channels are under investigation.

For current MIMO technologies, only the horizontal plane is utilized, i.e., linear antenna array with dual-polarization elements is usually deployed in the horizontal plane or sometimes different antenna elements deployed in the vertical plane are still only mapped to one antenna port and carry the same signal. Since there are no difference in the vertical dimension, these vertically distributed elements within an antenna port actually appear as one single antenna at the receive side [4]. We call this kind of MIMO with only different signals in horizontal plane as 2-dimensional (2D) MIMO. With the development of active antenna system, one promising way for further taking advantage of MIMO technique is to regard every element inside an antenna port as independent and feed it with different signals, such that the scale of MIMO can be extended to the vertical plane. Antenna arrays configured in this way at the base station (BS) are termed as 3-dimensional MIMO (3D MIMO) or full dimensional MIMO (FD-MIMO).

Recently, 3D MIMO has been identified as an important technique for throughput enhancement in LTE Release 12 for 3rd Generation Partnership Project (3GPP) and is attracting interest from researchers worldwide. In a recent research [5], performance comparison results between 3D MIMO and 2D MIMO are presented in ITU UMi scenario. In [6, 7], the characteristics and performance of FD-MIMO with various BS antenna configurations are studied. All of the above are based on the 3D spatial channel model (3D SCM) which combines 2D SCM with the vertical dimension parameters reported in WINNER+. However, it is not an accurate and verified 3D channel model [1]. From January 2013, a large effort has been being made within 3GPP to produce reliable 3D channel models and yet no standardized 3D MIMO channel model has been issued [4]. Besides, many theoretical analysis work on 3D MIMO are conducted in [8, 9]. In fact, using field channel measurement data to evaluate system performance is reliable and necessary. Various such 2D MIMO research works have been published [10, 11]. But to the best of the authors' knowledge, 3D MIMO performance evaluation based on real channel data has never been performed so far.

In this study, MIMO channel is measured in a typical urban high rise environment where the 3D MIMO is likely to be deployed [4, 6]. Using the measurement data, the performance of different 3D antenna settings are calculated for single-user MIMO (SU-MIMO) and multi-user MIMO (MU-MIMO) using perfect precoding and linear minimum mean square error (MMSE) precoding respectively. To find the optimal antenna configuration for SU-MIMO, the capacity of four different antenna settings with various antenna orientations and spacing are presented and analyzed. For MU-MIMO, the sum rates of different antenna configurations are calculated under different user distribution cases. On this basis, the relationship between user distribution and antenna setting is discussed. Moreover, the effect of increasing BS antenna number is also evaluated by comparing the sum rates under different BS antenna numbers. Finally, MU-MIMO sum rates are also calculated with different user numbers to check the influence of increasing user number on performance.

The paper is organized as follows. In Sec. II we describe our system model for the evaluation. Sec. III contains our field measurement description and 3D antenna configurations. The numeric results and relevant analysis are presented in Sec. IV before we conclude the paper in Sec. V.

II. SYSTEM MODEL FOR EVALUATION

Consider a single-cell 3D MIMO downlink system consisted of one base station equipped with N_t transmit antenna ports and K user equipments each with N_r receive antennas. We model the MIMO channel as a flat-fading channel on a single subcarrier. The k th user's channel matrix is denoted as $\mathbf{H}_k \in \mathcal{C}^{N_r \times N_t}$, and we assume that \mathbf{H}_k is available at the transmitter. The received signal vector by user k can be represented as

$$\mathbf{y}_k = \mathbf{H}_k \mathbf{z} + \mathbf{n}_k, k = 1, 2, \dots, K, \quad (1)$$

where $\mathbf{z} \in \mathcal{C}^{N_t \times 1}$ is the transmitted signal vector across the N_t transmitting antennas, and \mathbf{n}_k is an $N_r \times 1$ additive noise vector with independent and identically distributed random entries satisfying $\mathcal{CN}(0, \delta^2)$. Suppose the number of simultaneously transmitted parallel data streams to the k th user is $L \leq \min(N_t, N_r)$, the effective $L \times 1$ transmitted data symbol vector for the k th user is \mathbf{b}_k , which satisfies $E\{\mathbf{b}_k \mathbf{b}_k^H\} = \mathbf{I}_L$ and $E\{\mathbf{b}_k\} = 0$. To exploit the space dimension flexibility of multi-antenna system, precoding operation is performed. We assume that $\mathbf{P}_k \in \mathcal{C}^{N_t \times L}$ and $\mathbf{D}_k \in \mathcal{C}^{L \times N_r}$ are the precoder and decoder matrix for k th user, respectively.

For single-user MIMO, the precoded signals for the k th user are mapped directly to N_t transmitting antennas though \mathbf{P}_k , the received signal can be rewritten as

$$\mathbf{y}_k = \mathbf{H}_k \mathbf{z} + \mathbf{n}_k = \mathbf{H}_k \mathbf{P}_k \mathbf{b}_k + \mathbf{n}_k. \quad (2)$$

The singular value decomposition (SVD) of $\mathbf{H}_k^H \mathbf{H}_k$ is $\mathbf{H}_k^H \mathbf{H}_k = \mathbf{V}_k \mathbf{\Lambda}_k \mathbf{V}_k^H$. The ordered diagonal elements of $\mathbf{\Lambda}_k$ are $\chi_{\max} = \chi_1 \geq \dots \geq \chi_{N_t} = \chi_{\min} = 0$. From [11], we know that, when the optimal precoding matrix $\mathbf{P}_k^{opt} = \mathbf{V}_k^L$ is utilized, which is the first L columns of \mathbf{V}_k , the single-user capacity can be represented as

$$C_{su} = \sum_{l=1}^L \log_2 \left(1 + \frac{\gamma}{L} \chi_l \right), \quad (3)$$

where γ is the received SNR.

For multi-user MIMO, we assume that the number of simultaneously served users is $M > 1$, the precoded signals for all the M users are first added up together and then mapped to the N_t transmit antennas. The received signal of the k th user becomes

$$\mathbf{y}_k = \mathbf{H}_k \sum_{j=1}^M \mathbf{P}_j \mathbf{b}_j + \mathbf{n}_k. \quad (4)$$

At the receiving side, \mathbf{y}_k is passed through decoder and the output data vector $\hat{\mathbf{y}}_k$ can be expressed as $\hat{\mathbf{y}}_k = \mathbf{D}_k \mathbf{y}_k$. Through the iterative procedure based on MMSE criterion in [12] we can get the optimal precoders \mathbf{P}_k^{opt} and the corresponding decoders \mathbf{D}_k^{opt} of the k th being served users. Then the sum rate of the M users can be obtained as

$$S_{mu} = \sum_{k=1}^M \log_2 \det \left(\mathbf{I} + \frac{\mathbf{H}_k \mathbf{P}_k^{opt} (\mathbf{P}_k^{opt})^H \mathbf{H}_k^H}{\sum_{i=1, i \neq k}^M \mathbf{H}_k \mathbf{P}_i^{opt} (\mathbf{P}_i^{opt})^H \mathbf{H}_k^H + \delta^2 \mathbf{I}} \right). \quad (5)$$

III. MEASUREMENTS DESCRIPTION AND 3D ANTENNA CONFIGURATIONS

It can be seen from the capacity and sum rate expressions above that the key factor of the performance evaluation is to obtain channel response. In this section we give the process to get 3D channel response from measured channel matrix in a representative high rise scenario.

A. Measurement Description

The field measurement is carried out in a business district area of Beijing in the city center. The layout of the high rise propagation scenario is illustrated in Fig. 1. The BS is



Fig. 1. The layout of high rise propagation scenario.

installed on the top of a 11-floor building and transmitter (Tx) antenna height is 46 m above the street level. The receiving measurement spots are mainly planned in a 22-floor building near BS. This measurement is conducted on the 6th, 8th, 11th, 18th, 21st floor and the height of them are 21.8 m, 29.4 m, 41 m, 60.6 m, 72.4 m respectively. In every floor, the receiver (Rx) is placed on the trolley with a height of 1.78 m above the floor ground. Fig. 2 (a) and (b) show the view and environment of the Rx side, which is typical indoor open office scene.



(a) View of Rx



(b) Open Indoor Office

Fig. 2. View and environment of the Rx side.

To capture real channel response, the Elektrobit PropSound Channel Sounder is used during the measurement operating at the center frequency of 3.5 GHz with 100 MHz effective bandwidth. As described in detail in [2], the sounder which transmits periodic pseudo random binary signals works in a time-division multiplexing mode. The interval within which all transceiving antenna pairs are sounded once is defined as a measurement cycle. An omnidirectional array (ODA) consisting of 28 pairs of dual-polarized antennas is

implemented at the Rx, and 2D uniform planar array (UPA)

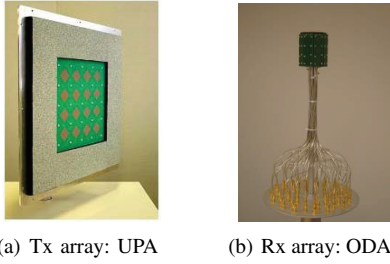


Fig. 3. Schematic sketches of antenna arrays.

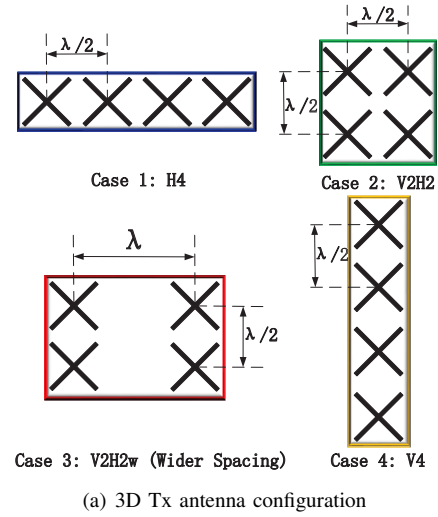
with half wavelengths spacing (0.5λ) consisting of 4 pairs of dual-polarized antennas both in the horizontal direction and the vertical direction is employed at the BS. The schematic sketches of the antenna arrays at Tx side and Rx side are shown in Fig. 3.

Through the measurement and channel sounding data pre-processing the channel matrix $\mathbf{H}(t, f, s, u)$, a natural 3D space propagation channel response, can be get. The variable t donates time, when one measurement cycle is measured, f is the subcarrier frequency, s is the s th Rx antenna element and u is the u th Tx antenna element. Since the 3D channel response between every transceiving antenna element pair is available, each antenna element can be treated as an independent antenna port.

B. 3D Antenna Configuration

In 3D MIMO system, the BS antennas are more likely to be placed in a 2D planar array [7]. In this research, four kinds of 3D antenna configurations, as illustrated in Fig. 4(a) with different dual-polarized antennas spatial positions in the 2D plane, are considered to check the performance of 3D MIMO. For Case 1, we refer the eight-antenna setup composed of horizontally distributed 4 pairs of closely spaced dual-polarized antennas as H4, which is prioritized in the LTE-Advanced MIMO design [3]. The spacing between two neighboring co-located dual-polarized antennas in H4 is 0.5λ . For case 2, the antenna array consisting of 2 pairs of dual-polarized antennas both in the vertical direction and horizontal direction is referred as V2H2 with 0.5λ spacing in both the vertical and horizontal dimension. Compared with case 2, we refer the antenna configuration in case 3 as V2H2w for the wider spacing (1λ) in horizontal dimensional. Similarly, the configuration in case 4 is referred as V4 with 0.5λ spacing for the vertically distributed four pairs of dual-polarized antennas. Every antenna element inside the four configurations is assumed as active antenna.

Since the two-dimensional UPA with 32 antennas is used at BS in the measurement, the four 3D antenna configurations can be built through antenna sub arrays selections at the UPA. In Fig. 4(b), we give one kind of subset array selection at UPA for the 3D transmitter realization. In fact, there are 4, 9, 6, and 4 kinds of different antenna groups to realize the 3D transmitter case 1, case 2, case 3, and case 4, respectively.



(a) 3D Tx antenna configuration

1/2	3/4	5/6	7/8
9/10	11/12	13/14	15/16
17/18	19/20	21/22	23/24
25/26	27/28	29/30	31/32

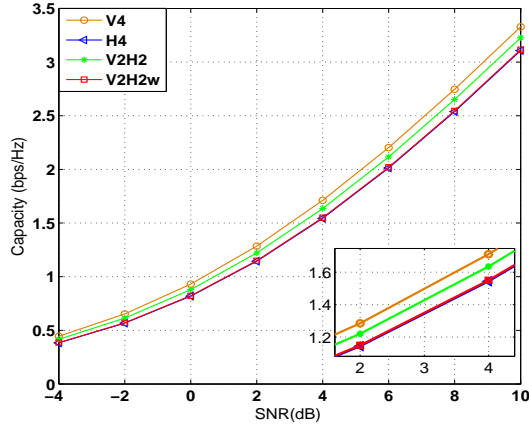
(b) Subset array selection at UPA

Fig. 4. 3D Tx antenna Configuration and one corresponding illustration of subset selection at UPA.

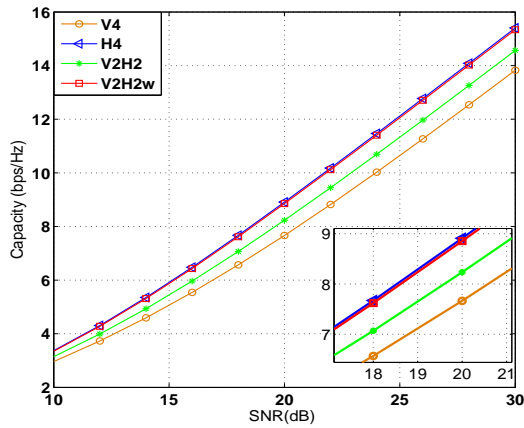
Similar to the Tx side, at the Rx a sub array selection is also introduced. We consider the mobile station equipped 2 receiving antennas, which are typical co-located dual-polarized antennas. The pair of dual-polarized antennas with the largest receiving energy among the 28 pairs of dual-polarized antennas at ODA is selected to represent a 2-antenna user terminal. After the procedure above, channel response matrix of the four 3D transmitters can be extracted from the measured channel data $\mathbf{H}(t, f, s, u)$. In next section, the performance is the average result performed over time t and frequency f , and also over all kinds of the different antenna groups for each antenna configuration.

IV. MEASUREMENT-BASED RESULTS AND ANALYSIS

Based on the measured high rise MIMO channel response, comparisons among the above four 3D MIMO antenna configurations are made in terms of SU-MIMO channel capacity with perfect precoding and MU-MIMO sum rate with linear MMSE precoding. Specially, the case that users distributed in different floors is first considered to form MU-MIMO channel for performing spatial separation in elevation dimension. Furthermore we present the sum rates of MU-MIMO in two-user case as the transmitting antennas increases and the performance of high order MU-MIMO when the BS is equipped with 32 antennas.



(a) Transmit Beamforming



(b) Spatial Multiplexing

Fig. 5. Single-user capacity for four 3D antenna configurations.

A. SU-MIMO

We plot the performance of single user MIMO with one layer transmission (Transmit Beamforming) in Fig. 5(a), which is usually applied to cell edge users with low SNR. While the performance of two layers transmission (Spatial Multiplexing) is plotted in Fig. 5(b) which higher SNR UEs tend to use. From Fig. 5(a), we can see that the capacity of V4 is better than that of the other three cases. The capacity of V2H2w is almost the same with H4, which provides the worst beamforming performance. However, Fig. 5(b) shows completely opposite results compared to Fig. 5(a). H4 has the best capacity gain for spatial multiplexing transmission while V4 performs worst.

As we know, the angle spread ‘seen’ by a given pair of antennas depends on the plane which they are spaced in and the angle spread in the elevation dimension is less than the azimuth dimension [2]. What’s more, bigger angle spread is more likely to form independent multiple streams of data to a single user for multilayer transmission. This is because the bigger angle spread means stronger variation in the multipath components of different antennas, which results in

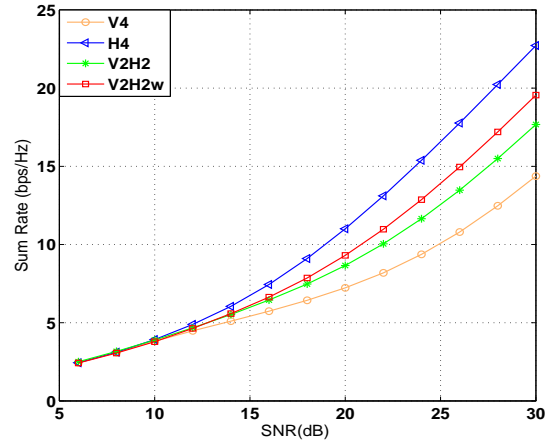


Fig. 6. Two-user sum rate with $d_V=0$ m, $d_H=16.4$ m.

weakened transmitted signal similarity or correlation across the antennas. Therefore H4 has better performance in spatial multiplexing for horizontally distributed antennas ‘see’ wider azimuth angle spread. However, in V4 antennas are distributed in the vertical plane, thus the smaller elevation angle spread is ‘seen’, which means higher antenna port correlation and better beamforming capability. V2H2 and V2H2w are somewhere in between V4 and H4 since their antennas are distributed both in the vertical dimension and the horizontal dimension. It needed to be noted that compared to V2H2, V2H2w performs better in spatial multiplexing and worse in transmit beamforming for wider spacing between two dual-polarized neighboring antennas leading to lower antenna correlation.

B. MU-MIMO

In this section, we extract the measured data in different measurement positions to form MU-MIMO channel responses. It is assumed that the BS serves multiple users and each user takes two spatial layers. Let d_V and d_H denote the vertical plane distance and horizontal plane distance between the two users. Since the benefits of MU-MIMO are most significant for UEs with medium-high SNR, the SNR here is kept in the range of 6 dB to 30 dB.

Fig. 6 shows the sum rate of the two users located in the same floor. It can be seen that H4 performs the best while V4 performs worst. This is because horizontally distributed antennas can form multi-beam to separate user spread across the azimuth dimension while the vertical configuration can only form beams to multiple users distributed in elevation direction. For similar reason, the sum rate of V2H2 and V2H2w are better than that of V4 but worse than H4. Comparing V2H2w with V2H2, we can find that when SNR is low the sum rate of V2H2w is slightly less than V2H2, but as SNR increases V2H2w outperforms V2H2 quickly. The main reason is that V2H2 is more suitable for beamforming for its relatively smaller antenna spacing, however, under higher SNR V2H2w performs better for its wider antenna spacing.

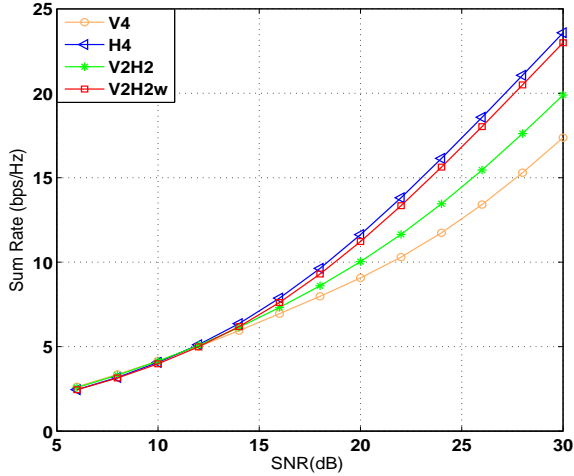


Fig. 7. Two-user sum rate with $d_V=19.6$ m and $d_H=21.3$ m.

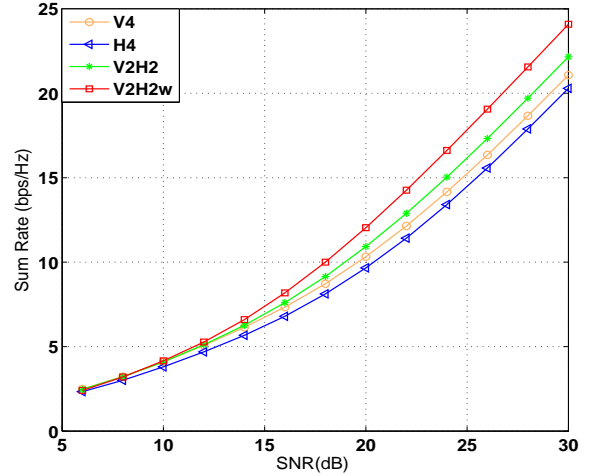


Fig. 9. Two-user sum rate with $d_V=50.6$ m and $d_H=1.2$ m.

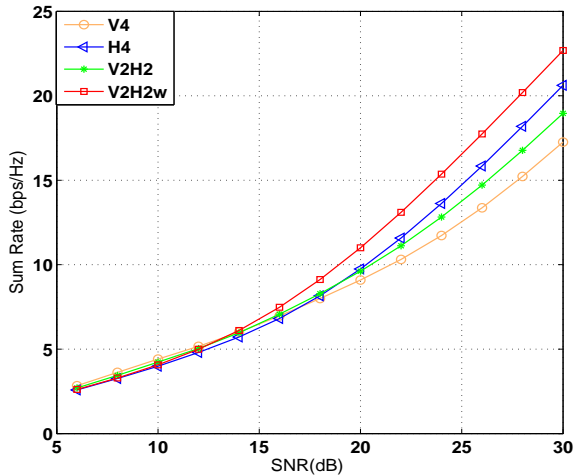


Fig. 8. Two-user sum rate with $d_V=19.6$ m and $d_H=1.2$ m.

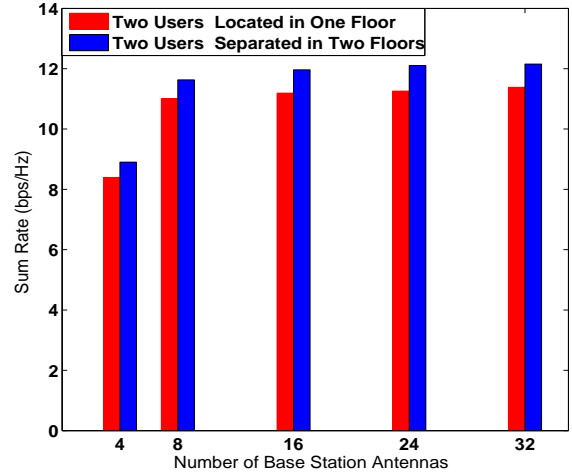


Fig. 10. Two-user sum rate for different number of BS antennas with $SNR=20$ dB.

Fig. 7 shows the sum rate of the two users located on different floors with a wider separation in horizontal plane. Since the two users are widely separated in both the vertical and horizontal level, each of the four 3D transmitters can form multi beams to serve them. However, for high SNR, H4 case and V2H2w still have better performance than V4 and V2H2. Because either the wider azimuth angle spread ‘seen’ by H4 or the wider spacing between horizontal domain antennas in V2H2w can better support multilayer transmission, which is consistent with the results in single-user multilayer transmission.

Furthermore, in Fig. 8 and Fig. 9, the sum rate results are plotted when the two users are located on different floors but have small horizontal separation. From Fig. 8, we can see that V4 configuration performs best under low SNR for its stronger ability to separate the two vertical separated users. However, as SNR increases, it becomes the worst for its small elevation angle spread which leads to poor ability of multilayer transmission. On the contrary, V2H2w configuration quickly

shows its advantage of combining the ability of separating vertically distributed users and good capability of multilayer transmission. Additionally, we find that though H4 performs worst in low SNR range, it still exceeds V4 and V2H2 in high SNR range due to its better ability of supporting multilayer transmission. But for the wider vertically separated users, H4 performs worst over the whole SNR scope for its disability to separate vertically distributed users in Fig. 9. Also in Fig. 9, V2H2w configuration shows best performance.

Combining the results in Fig. 7, Fig. 8 and Fig. 9, it can be observed although V2H2w doesn’t perform best when two users are separated in both the vertical and horizontal plane or when SNR is relatively low, but its performance is very close to the best. What’s more, except these two cases, V2H2w shows a significant performance advantage compared to the other three antenna configurations. So V2H2w antenna configuration is most suitable for the MU-MIMO when users are mainly vertically separated.

To study the performance of MU-MIMO under different

number of transmitting antennas, in Fig. 10, we give the two-user sum rates when the BS is equipped with 4, 8, 16, 24, 32 antennas respectively. We can see that the sum rates increase with the number of transmitting antennas, when the number of transmitting antennas increases from 4 to 8, the sum rates increase by 2.6 bps/Hz and 2.7 bps/Hz respectively. However, the rate of increase become marginal when the number of transmitting antennas exceeds 8. When the number of transmitting antennas is 32, the sum rates increase by only 0.4 bps/Hz and 0.6 bps/Hz compared to the 8 transmitting antennas case. It indicates that for two-user MU-MIMO, simply increasing the number of transmitting antennas may not bring significant performance gain. What's more, it is also found that the sum rates is larger when users are separated in two floors.

In Fig. 11, we give the sum rates in the case of increasing number of simultaneously served users when the BS is equipped with 32 antennas. For the users distributed in four floors case the sum rate of 8 users increases 57% compared to that of 2 users. The result reveals that when the BS is equipped with a big number of antennas realizing high order MU-MIMO indeed improves the overall performance than two-user case.

Also from Fig.11 we can observe that the performance of the served users distributed in four floors is better than the case in which users distributed in two floors and this is consistent with the result in Fig. 10. It indicates selecting users located in different floors for MU-MIMO system can achieve better performance since the users in different floors have lower channel correlation.

V. CONCLUSION

In this paper, the performance of SU-MIMO and MU-MIMO are analyzed on the basis of measurement in high rise scenario. Comparisons are conducted for four 3D antenna configurations. Analysis and Comparison results reveal that closely spaced vertical configuration does better in transmit beamforming while closely spaced horizontal configuration works better in spatial multiplexing for its wider angle spread in azimuth dimension. For multiple users each with multiple streams, when they are located on the same floor horizontally distributed antennas performs best while for users located on different floors, the configuration combining closely spaced vertically distributed antennas with widely spaced horizontally distributed antennas is a more suitable choice for its ability of both separating vertically distributed users and supporting multilayer transmission. At last, we observed that realizing high order MU-MIMO can improve the overall performance when the BS is equipped with a big number of antennas and selecting users located in different floors for 3D MU-MIMO system can achieve better performance. The conclusions may be helpful for the antenna selection and deployment of 3D MIMO in practical environments.

ACKNOWLEDGMENT

The research is supported by National Science and Technology Major Project of the Ministry of Science with 2013ZX03003016-005, National Natural Science Foundation

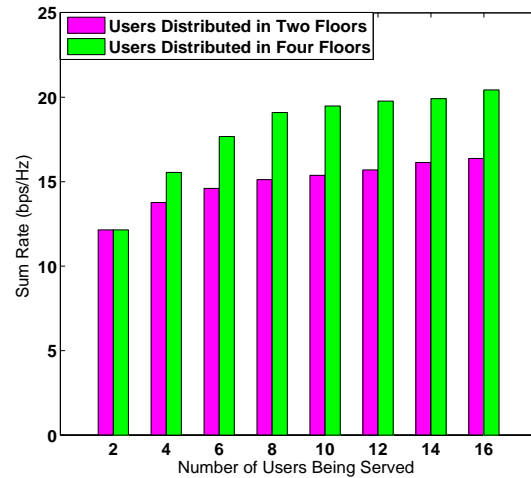


Fig. 11. Sum rates for different number of users with SNR=20dB when the BS is equipped with 32 antennas.

of China with No. 61171105, National 863 Project of the Ministry of Science and Technology with 2014AA01A705, Program for New Century Excellent Talents in University of Ministry of Education of China with NCET-11-0598.

REFERENCES

- [1] I. F. Akyildiz, D. M. Gutierrez-Estevéz, R. Balakrishnan, and E. Chavarria-Reyes, "LTE-Advanced and the Evolution to Beyond 4G (B4G) Systems," *Physical Communication (Elsevier Journal)*, in press, 2013.
- [2] J. Zhang, C. Pan, F. Pei, G. Liu, X. Cheng, "Three-dimensional fading channel models: A survey of elevation angle research," *IEEE Communications Magazine*, vol.52, no.6, pp.218-226, June 2014.
- [3] F. Boccardi, B. Clerckx, and A. Ghosh, "Multiple-antenna techniques in LTE-advanced," *IEEE Communications Magazine*, vol. 50, no. 3, pp. 114-121, March 2012.
- [4] K. Abla, H. Khanfir, Z. Altman, M. Debbah and M. Kamoun, "Survey on 3D channel modeling: From theory to standardization," *arXiv preprint arXiv:1312.0288* 2013.
- [5] Y. W. Pan, Q. L. Luo, G. D. Li, Y. Zhao and Z. L. Xiong, "Performance Evaluation of 3D MIMO LTE-Advanced System," Vehicular Technology Conference (VTC Fall), 2013 IEEE 78th, pp. 1-5, 2-5 Sept. 2013.
- [6] Y. S. Kim, H. J. Ji, H. Lee, J. H. Lee, B. L. Ng and J. Z. Zhang, "Evolution beyond LTE-advanced with Full Dimension MIMO," Communications Workshops (ICC), 2013 IEEE International Conference on, pp. 111-115, 9-13 June 2013.
- [7] Y. H. Nam, B. L. Ng, K. Sayana, Y. Li, J. Z. Zhang, Y. S. Kim and J. H. Lee, "Full-dimension MIMO (FD-MIMO) for next generation cellular technology," *IEEE Communications Magazine*, vol. 51, no. 6, Jun. 2013.
- [8] M. Dao, V. Nguyen, Y. Im, S. Park, G. Yoon, "3D Polarized Channel Modeling and Performance Comparison of MIMO Antenna Configurations With Different Polarizations," *Antennas and Propagation, IEEE Transactions on*, vol.59, no.7, pp. 2672-2682, July 2011
- [9] M. Shafi, M. Zhang, P. J. Smith, A. L. Moustakas, and A. F. Molisch, "The impact of elevation angle on MIMO capacity," IEEE International Conference on Communications, vol. 9, pp. 4155-4160, 2006.
- [10] C. Schneider, N. Iqbal and R. S. Thomä, "Performance of MIMO order and antenna subset selection in realistic urban macro cell," Personal Indoor and Mobile Radio Communications (PIMRC), 2013 IEEE 24th International Symposium on, pp. 992-996, 8-11 Sept. 2013
- [11] J. Gao, J. Zhang, Y. Xiong, Y. Sun and X. Tao, "Performance evaluation of closed-loop spatial multiplexing codebook based on indoor MIMO channel measurement," *International Journal of Antennas and Propagation*, vol. 2012, 2012.
- [12] J. Zhang, Y. Wu, S. Zhou and J. Wang, "Joint linear transmitter and receiver design for the downlink of multiuser MIMO systems," *IEEE Commun. Letters*, vol. 9, no. 11, pp. 991-993, Nov. 2005.